Available online at www.sciencedirect.com
SCIENCE DIRECT
Journal of Hydrology 313 (2005) 257–273
Journal of Hydrology
www.elsevier.com/locate/jhydrol

Single-porosity and dual-porosity modeling of water flow and solute transport in subsurface-drained fields using effective field-scale parameters

Nathan W. Haws[a,*], P. Suresh C. Rao[a,b], Jirka Simunek[c], Irene C. Poyer[a]

[a]School of Civil Engineering, Purdue University, West Lafayette, IN 47907-1150, USA
[b]Department of Agronomy, Purdue University, West Lafayette, IN 47907-2054, USA
[c]Department of Environmental Sciences, University of California, Riverside, CA 92521, USA

Received 28 July 2004; revised 14 March 2005; accepted 16 March 2005

Abstract

Water and solute flux from the subsurface drains of macroporous agricultural fields are simulated using two-dimensional single-porosity and dual-porosity models. Field-averaged (i.e. effective) parameters are calibrated from drainage outflow and validated for water flow and the transport of non-reactive solutes applied at discrete locations on the field. Both the single-porosity and the dual-porosity simulations capture the observed trends in the drainage hydrographs, with the dual-porosity model performing slightly better than the single-porosity model. The values of the effective hydrologic parameters, however, were not fully characteristic of macroporous soils. The physical meaning of the effective parameters was further questioned as neither the single-porosity nor the dual-porosity models could simulate the rapid transport of solutes to the subsurface drain. The discrepancies between the simulated and observed solute flux indicate that the actual spatial area contributing to drainage outflow in the field experiment was much greater than the integrated area of the simulated domain over which the effective parameters were calibrated. Supplementary simulations using parameters calibrated from solute flux data (outflow solute concentration multiplied by the outflow water flux) also fail to match both water and solute fluxes. The failure of the simulations is attributable to factors such as non-unique parameters and problems with representing a three-dimensional heterogeneous domain as a two-dimensional homogeneous system, including a misrepresentation of macropore flow paths. This study shows the fallacy of interpreting a hydrograph fit as evidence of the physical meaning of model parameters.

Keywords: Dual-porosity; HYDRUS-2D; Effective parameters; Subsurface-drains; Model calibration

1. Introduction

Agricultural landscapes consist of multi-scale heterogeneities that influence the movement of water and chemicals. Usually, a detailed quantification of spatial variability is either impractical or

* Corresponding author. Address: Department of Geography and Environmental Engineering, Johns Hopkins University, Baltimore, MD 21218-2686, USA. Tel.: +1 410 516 4255; fax: +1 410 516 8996.
E-mail address: nhaws@jhu.edu (N.W. Haws).

0022-1694/$ - see front matter © 2005 Elsevier B.V. All rights reserved.
doi:10.1016/j.jhydrol.2005.03.035

impossible. Consequently, models for predicting flow and transport through the vadose zone must somehow simplify the representation of the transport domain, yet still effectively reproduce the flow and transport response at a control plane or outlet point. In a deterministic model, this is often accomplished by assuming a representative elementary volume (REV), which proposes that a medium can be represented by homogenized (i.e. effective) parameters provided there is a separation of scales such that the characteristic volume of spatial heterogeneities is much smaller than macroscopic size of the transport domain (Royer et al., 2002).

The REV assumption is commonly invoked to calibrate effective model parameters from catchment outflow hydrographs for rainfall-runoff models. Often the legitimacy of these models is validated solely on the basis of hydrograph prediction (Beven, 1993; Beran, 1999). Using the outflow response as an exclusive measure of performance, however, is being increasingly questioned as these models fail to represent the actual drainage pathways and the physical processes occurring within the flow domain (Binley et al., 1991; Jain et al., 1992; Blazkova et al., 2002). Consequently, models become more sophisticated to better account for the internal system structure. The increased sophistication results in increased parameterization requirements. Because it is typically infeasible to make detailed distributed measurements, the added parameters must be estimated based on the same hydrograph information, which leads to a higher likelihood of non-unique parameter sets and an ill-posed inverse calibration problem—even for simple, small-scale systems (Hopmans and Šimůnek, 1997; Durner et al., 1997; Madsen et al., 2002; Doherty and Johnston, 2003).

While the REV approach to finding effective parameters is simple in concept, verifying its existence can be complicated. (Baveye and Sposito, 1984; Berkowitz et al., 1988; Neuman and Orr, 1993; Lugo et al., 1998; Tartakovsky and Neuman, 1998a,b,c; Indelman, 2002; Fernandez-Garcia et al., 2002; Royer et al., 2002). Neuman and Orr (1993) demonstrated mathematically that while effective values may be found for infinite subsurface domains, the flux for bounded systems becomes non-local, and thus, an average flow model generally does not exist. For radially converging flow systems, however, they showed that effective parameters could be found depending on the correlation structure and physical dimensions of the domain.

Temporal variability also creates difficulties in finding effective parameters. Tartakovsky and Neuman (1998b) reported that for porous media, an effective hydraulic conductivity will exist in the 'strict sense' only when the mean head and the residual flux are constant in space and time. Though this is not possible under transient flow—except if the storativity is zero or time approaches infinity—there are a number of cases, where effective hydraulic conductivities can be approximated in real, Laplace and/or Fourier spaces (Tartakovsky and Neuman, 1998b,c).

Some of the more complex flow and transport domains are subsurface-drained agricultural fields of the US Midwest region. Analogous to catchment hydrographs, the subsurface drain response is an aggregation of the spatial and temporal variability across that part of the field that contributes to drainage outflow. Consequently, the drainage hydrograph may be useful for estimating effective parameters if the transport domain can be approximated as a radially converging flow system, spatial correlation lengths of variability in the soil properties are small compared to the field dimensions, and rainfall events are limited to a realistic range of magnitudes such that the field volume contributing to the outflow does not appreciably change between events. Still, even when these conditions are met, the non-linear processes in the vadose zone, coupled with flow and transport through macropore networks that are abundant in these soils, may violate the ergodic hypothesis (Yeh, 1997) and the representations of the driving processes.

As in catchment modeling, using the outlet response to derive effective hydraulic properties for subsurface-drained fields is not new (Hoffman and Schwab, 1964; Skaggs, 1976), and automated inverse procedures have been developed and tested for a variety of systems of different scales and for a number of boundary conditions (Durner et al., 1997; Hopmans and Šimůnek, 1997; Jacques et al., 1997; Šimůnek et al., 1998). De Vos et al. (1997) used the inverse procedure in the HYDRUS-2D flow and transport model to estimate effective field-scale parameters from measurements of drainage outflow and groundwater level fluctuations. The effective parameter model could satisfactorily reproduce the overall

water balance and the observed water fluxes; however, it failed to predict the rapid arrival at the drain outlet of a bromide tracer that was surface applied to the field. De Vos et al. (1997) attributed the model's failure in the solute simulations to the soil macropores that created a preferential transport domain that was not well described by a single saturated hydraulic conductivity value. They further surmised that a more complex, dual-domain model would better simulate solute transport. More recently, Gerke and Köhne (2004) modeled the one-dimensional leaching of bromide in a subsurface-drained field using both the single-porosity HYDRUS-1D model and a one-dimensional dual-porosity/dual permeability (i.e. two mobile domains) model. Again, they found that both models could satisfactorily explain water flow, yet only the dual-permeability model could reproduce the bromide concentrations in the outflow.

With the supposition that the subsurface-drain integrates field-scale heterogeneity, this study follows the work of De Vos et al. (1997) and Gerke and Köhne (2004) by using a version of the HYDRUS-2D code (Šimůnek et al., 1999) that was modified to include a dual-porosity/single-permeability (i.e. mobile–immobile) flow and transport domain (Šimůnek et al., 2003). Furthermore, the solute simulations are conducted for tracers applied on discrete locations of the field, so that the solute concentrations in the drainage signal a two-dimensional field location and transport pathway. Effective parameters are calibrated for both single- and dual-porosity models based on subsurface-drainage outflow data. The effective parameter models are then evaluated for both water and solute flux. The objectives of these modeling studies is to evaluate effective hydraulic parameters that are calibrated based on drainage data, to assess the benefits of increasing model complexity (single- vs. dual-porosity), and to test the physical representativeness of parameters by their ability to simulate solute flux and reproduce the contributing drainage areas the flow domain.

2. Field experiments

Replicate multi-solute experiments were conducted on two subsurface-drained cornfield plots (labeled Plots 51 and 52) at the Purdue Agronomy Water Quality Field Station (WQFS), West Lafayette, Indiana. The soil at the field station is classified as Drummer silty clay loam (fine-silty, mixed mesic Typic Endoquoll), has a primarily sub-angular blocky structure in the upper 2 m profile, and an A horizon that typically extends to at least 40 cm (USDA, 1998). Although the soil is classified as poorly drained, macropores that are formed by root channels, earthworm burrows, and other bio-processes can rapidly convey water and solute from the soil surface to the drain outlet.

Plots 51 and 52 each measure $48.5 \times 60\ m^2$ ($L \times W$), with crop rows running along the 48.5 m length, parallel to the subsurface drain. Each plot is also drained by two perimeter drains and a central drain that bisects the perimeter drains, giving a 30 m horizontal drain spacing. The subsurface drains are approximately 1 m below the ground surface, and a relatively impermeable glacial till lies at about 2 m below ground. The central subsurface drain of each plot routes effluent to collection huts equipped with tipping bucket flow meters and automatic water sampling devices. Bucket tips were recorded with data loggers (Campbell Scientific, Model CR510), triggered via a magnetic sensor switch located on the bottom of the tipping bucket. Drainage effluent was sampled with automatic samplers (ISCO, Model 3700) that were programmed to draw a 300 ml water sample every 100 tips of the bucket meter (approximately 130 l depending on the specific tipping bucket calibration). The flow-weighted sampling provided a greater sampling intensity during storm peaks and reduced sampling frequencies during the hydrograph recessions. The 300 ml samples were sub-sampled in 40 ml volatile organic vials, and stored at 4 °C until analyzed.

The experiments were conducted under natural rainfall and atmospheric conditions. Rainfall and evaporation values, used as input boundary fluxes in the HYDRUS-2D model, were obtained from measurement locations at or near the field site. Hourly rainfall amounts were recorded with two rain gauges located at the field site. Daily evaporation values were measured from a Class A evaporation pan located about 0.8 km south of the field plots.

A water budget was computed to verify that the measured rainfall, evaporation, and drainage outflow

accounted for all the water fluxes to and from the plots. For the water budget, a constant pan factor of 0.7 was used to adjust the potential evaporation values measured in the Class A pan to actual field evaporation values. It should be noted that in reality, pan factors are not constant, but can vary from about 0.35, for dry conditions, to about 0.85, for very wet/humid conditions, and the factor of 0.7 is an average value suggested by Brouwer and Heibloem (1986). Another complication with computing the water budget is that no water content data were available so that there could be no direct accounting for the change in water storage within the flow domain. Consequently, the water budget computations began at the cessation of drainage so that the initial soil condition could be assumed to be at hydrostatic equilibrium, and only boundary fluxes (rainfall, evaporation, and drainage) were considered in the water budget calculations. The cumulative water budget is shown in Fig. 1. In this figure, water fluxes entering the domain (rainfall) are taken as negative values, and water fluxes leaving the domain (outflow and evaporation) are positive. Theoretically, a budget value of zero at the end of a drainage event (i.e. when the soil again reaches hydrostatic equilibrium) means a perfect balance between inflow and outflow fluxes. In general, a good water balance is achieved before and after mid-May. The larger negative errors during mid-May indicate a likely underestimation of evaporation (or underestimation of the pan factor) from about May 10–25. (Note, that any underestimate cannot be attributed to an additional demand from cropwater uptake since corn was not planted until June.) Some of the imbalance in the budget also may result from changes in water storage that were not explicitly considered.

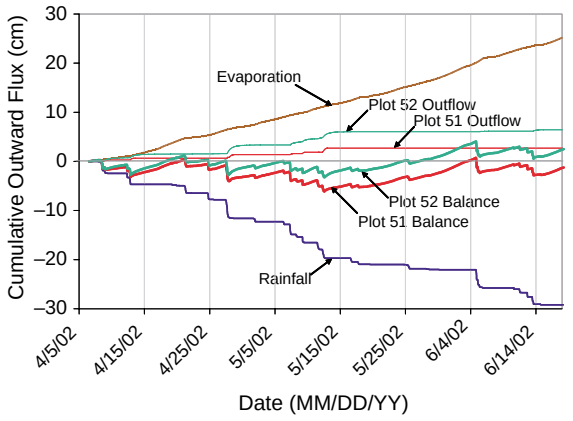

Fig. 1. Cumulative water fluxes for rainfall, evaporation, and drainage for Plots 51 and 52. Also shown is the water balance for Plots 51 and 52, computed as rainfall + evaporation + outflow. Water flux out of the domain is taken as positive.

The field experiments began in April, 2002. Prior to the solute application, potassium chloride and potassium bromide were dissolved individually in water, and stored separately. On April 6, 2002, the concentrated solutions were surface applied to separate 1 m wide 'strips' that ran parallel to the subsurface drain. The chloride solution was applied to a 1 m wide strip centered at a lateral offset of 0.5 m from the drain. The bromide solution was applied to a 1 m wide strip centered 5 m from the drain. The strip widths were chosen based on two criteria: (1) to be thin enough so that solute outlet response would signal a distinct field origin, and (2) wide enough to allow a convenient and accurate solute application. Although both Plots 51 and 52 have drain half-spacing of 15 m, the outer strip was centered only 5 m from the subsurface drain in order to negate any boundary effects and prevent the chance of solute capture in the perimeter drains. Several spray passes were made along the length of each strip to ensure uniform tracer application. For each application, the spray nozzle was kept close to the soil surface to minimize drift of the spray droplets. To prevent cross-contamination, different backpack sprayers were used for each tracer mixture. Water flux and solute concentration in the drain outflow were monitored through the end of 2002; however, only data obtain prior to the planting date of June 3, 2002 were used in the modeling study.

Chloride and bromide concentrations in the drain effluent samples were analyzed utilizing a Dionex DX600 Ion Chromatography system, equipped with an ED50 electrochemical detector, an AG40 potassium hydroxide eluent generator, a GP50 pump, and an AS50 autosampler. Analytes were separated using a Dionex IonPac 4×50 mm guard column in tandem with an IonPac AS17 4×250 mm analytical column and a potassium hydroxide eluent gradient ramped from 12 to 25 mM. Background anion suppression was maintained to less than 2.0 μS (micro-Siemens) with an ASRS Ultra 4 mm suppressor. The method detection limit was 0.25 mg/l.

3. Flow and transport modeling and parameter estimation

Flow and transport simulations were conducted with the HYDRUS-2D finite-element code (Šimůnek et al., 1999), modified to include a dual-porosity/single-permeability module (Šimůnek et al., 2003). The finite-element grid was constructed to represent a two-dimensional, vertical section of the WQFS plots (Fig. 2). The modeled field domain was 15×2 m^2 (width$\times$depth), assuming symmetry about the vertical plane of the drain and a no-flux boundary at the midplane between the central and perimeter drains. For the water flow simulations, the field was represented with 60×43 finite element cells with a cell spacing that tapered toward the drainage outlet located at $z=100$ cm at the right end of the domain. This mesh configuration was sufficiently refined to give mass balance errors of less than one percent for water flux. The sides and bottom of the domain were specified as no-flux boundaries, and the top of the domain had an atmospheric boundary. The subsurface drain was represented as a nodal sink (Šimůnek et al., 1999) with an effective drain diameter, d_e, of 1 cm and a reduction of hydraulic conductivities of the square in the finite element mesh surrounding the drain using the correction factor, C_d, of four (Mohammad and Skaggs, 1983; Fipps et al., 1986).

In the single-porosity model, the entire flow domain conducts water according to Richards' equation and transports solute according to the advection–dispersion equation.

Water:

$$\frac{\partial\theta}{\partial t}=\nabla[K(h)\nabla(h-z)] \tag{1a}$$

$$q=-K(h)\nabla(h-z) \tag{1b}$$

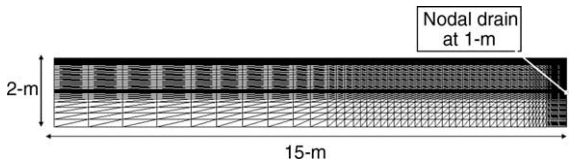

Fig. 2. The HYDRUS-2D finite element mesh used in the water flow simulations.

$$K(h)=K_s\left(\frac{\theta-\theta_r}{\theta_s-\theta_r}\right)^{\frac{1}{2}}\left\{1-\left[1-\left(\frac{\theta-\theta_r}{\theta_s-\theta_r}\right)^{\frac{n}{n-1}}\right]^{\frac{n-1}{n}}\right\}^2 \tag{1c}$$

$$\begin{aligned}\theta&=\frac{\theta_s-\theta_r}{[1+|\alpha h|^n]^{1-(1/n)}}+\theta_r \quad \text{for } h<0\\ \theta&=\theta_s \quad \text{for } h>0\end{aligned} \tag{1d}$$

Solute:

$$\frac{\partial}{\partial t}(\theta C)=\nabla(D\nabla C-qC) \tag{2a}$$

$$D=D_0+\lambda\frac{q}{\theta} \tag{2b}$$

where θ[L^3/L^3] is the water content (subscripts s and r denote saturated and residual, respectively), K [L/T] is the hydraulic conductivity, h [L] is the pressure head, α [1/L] and n [−] are the van Genuchten (1980) pressure-saturation parameters, and t [T] and z [L] are temporal and spatial coordinates (z positive downward), respectively. Also, C [M/L^3] is the aqueous solute concentration, q [L/T] is the water flux, and D is the hydrodynamic dispersion coefficient [L^2/T], which is defined by the dispersivity, λ [L], and the diffusion coefficient, D_0 [L^2/T].

The dual-porosity model divides the flow domain into mobile (subscript m) and immobile (subscript im) regions with first-order advection and diffusion between the two domains (Šimůnek et al., 2003).

Water:

$$\frac{\partial\theta_m}{\partial t}=\nabla\left[K(h_m)\nabla\left(h_m-z\right)\right]-\Gamma_w \tag{3a}$$

$$\frac{\partial\theta_{im}}{\partial t}=\Gamma_w \tag{3b}$$

$$q=-K(h_m)\nabla(h_m-z) \tag{3c}$$

$$\Gamma_w=\omega_w(h)(h_m-h_{im}) \tag{3d}$$

Solute:

$$\frac{\partial}{\partial t}(\theta_m C_m)=\nabla(D_m\nabla C_m-q_m C_m)-\Gamma_s \tag{4a}$$

$$D_m=D_{m0}+\lambda_m\frac{q_m}{\theta_m} \tag{4b}$$

$$\frac{\partial}{\partial t}\left(\theta_{\mathrm{im}} C_{\mathrm{im}}\right) = \Gamma_{\mathrm{s}} \tag{4c}$$

$$\Gamma_{\mathrm{s}} = \Gamma_{\mathrm{w}} C^{*} + \omega_{\mathrm{s}}(C_{\mathrm{m}} - C_{\mathrm{im}}) \tag{4d}$$

where Γ_{w}[1/T] is the water transfer term, Γ_{s} [M/L^{3}T] is the solute transfer term and $C^{*}=C_{\mathrm{m}}$ for $\Gamma_{\mathrm{w}}>0$ and C_{im} for $\Gamma_{\mathrm{w}}<0$. The solute transfer rate coefficient, ω_{s} [1/T], is a constant that accounts for the diffusive solute transport due to concentration gradients. The water transfer rate coefficient, ω_{w} [1/LT], is defined as follows (Gerke and van Genuchten, 1993; Šimůnek et al., 2003):

$$\omega_{\mathrm{w}}(h) = \frac{\beta}{d^2} K_{\mathrm{a}}(h)\gamma_{\mathrm{w}} \tag{5}$$

where β [−] is a geometric shape factor, d [L] is the characteristic length of the soil matrix, γ_{w} [−] is a scaling coefficient, and K_{a} is the effective hydraulic conductivity of the fracture–matrix interface, calculated using Eq. (1c) with immobile zone retention parameters. K_{a} is commonly defined as an arithmetic average involving both h_{m} and h_{im} as follows (Gerke and van Genuchten, 1996):

$$K_{\mathrm{a}}(h) = 0.5[K_{\mathrm{m}}(h_{\mathrm{m}}) + K_{\mathrm{im}}(h_{\mathrm{im}})] \tag{6}$$

In HYDRUS-2D, ω_{w} is a lumped coefficient that combines all the right-hand side terms in Eq. (5). The input value for ω_{w} is based on K_{a} at soil saturation, and the actual value of ω_{w} varies with pressure/saturation level according to Eq. (3d).

Five parameters are needed to describe the variably saturated water flow in the single-porosity domain: saturated water content (θ_{s}), residual water content (θ_{r}), the van Genuchten (1980) soil–water characteristic parameters (α, n), and the saturated hydraulic conductivity (K_{s}). Water flow in the dual-porosity model requires the same parameters as in the single-porosity model in the mobile region plus five other parameters for the immobile region: θ_{sim}, θ_{rim}, α_{im}, n_{im}, and ω_{w}. The additional parameters of the dual-porosity model, while complicating the inverse procedure, were expected to better represent the macropore flow processes than the single-porosity model.

To find and test the effective hydraulic parameters, the field data were parsed into two sections. The first section, used for calibration, began on April 3 at 0:00 h for Plot 51 and April 6 at 12:00 h for Plot 52 and ended on April 23 at 19:00 h for both plots—a total of 500 and 416 h for each plot, respectively. The beginning dates and times were selected to correspond to the completion of a previous drainage event for each of the plots to justify the initial condition of a horizontal water table located at the drain invert and hydrostatic equilibrium within the domain. The rainfall–evaporation–outflow data used for parameter validation began at the ending date and time of the calibration sets and continued until just prior to the planting date on June 3, 2002 (results are only shown up to May 24, 2002 since no drainage events occurred after this date). Ideally, a longer data set would have been chosen for model calibration; however, experimental data for water and solute were simultaneously available only for the 2002 season. It is possible that performing the calibration over a longer period would lead to different parameter values; nevertheless, the two rainfall events in the calibration period and the drying interlude between the events provide a good range of transient conditions for estimating the model parameters.

Parameters were calibrated using the inverse module within the HYDRUS-2D software package. HYDRUS-2D employs the Marquart–Levenberg optimization algorithm to aid in finding best-fit parameters. The objective of this routine is to minimize the sum of the squared deviations (SSD) between the observed and simulated drainage outflow values. In addition to using the minimum SSD objective, the parameter sets were also evaluated with the correlation coefficient

$$\rho_{x,y} = \frac{[\mathrm{COV}(x,y)]}{[\sigma_x][\sigma_y]} \tag{7}$$

where COV is the covariance functions, σ is the standard deviation, and x and y are the observed and simulated outflows, respectively. The additional use of the correlation coefficient was helpful as an indication of how well the model predictions matched the timing and general shape of the observed water and solute outflow fluxes while the SSD was used as a measure of the distance between simulated and observed outflow fluxes.

In the inverse procedure, all parameters were calibrated except the residual water content for

Table 1
Range of parameter values for (a) single-porosity and (b) dual-porosity models

Parameter	Value or range	Definition
(A)		
θ_r	0.07–0.2 (cm^3/cm^3)[a]	Residual water content
θ_s	0.3–0.6 (cm^3/cm^3)[a]	Saturated water content
α	0.003–0.4 (1/cm)	Water retention parameter (van Genuchten, 1980)
n	1.01–6 (−)	Water retention parameter (van Genuchten, 1980)
K_s	1–2000 (cm/h)	Saturated hydraulic conductivity
D_p	1 (cm^2/h)	Diffusion coefficient
λ_L, λ_T	15, 1.5 (cm)	Longitudinal, tranverse dispersivity
(B)		
θ_{rm} (mobile)	0	Residual water content in the mobile (macropore) domain
θ_{sm} (mobile)	0.01–0.15 (cm^3/cm^3)[b]	Saturated water content in the mobile (macropore) domain
α_m(mobile)	0.003–0.4 (1/cm)	Water retention parameter in mobile domain
n_m(mobile)	1.01–6 (−)	Water retention parameter in mobile domain
K_s	1–2000 (cm/h)	Saturated hydraulic conductivity
θ_{rim} (immobile)	0.07–0.2 (cm^3/cm^3)	Residual water content in the immobile (matrix) domain
θ_{sim} (immobile)	0.25–0.45 (cm^3/cm^3)	Saturated water content in the immobile (matrix) domain
α_{im} (imsmobile)	0.003–0.4 (1/cm)	Water retention parameter in the immobile domain
n_{im} (immobile)	1.01–5 (−)	Water retention parameter in the immobile domain
ω_w	0–0.1 (1/cm-h)	First-order advective exchange term
ω_s	0–0.1 (1/h)	First-order diffusion exchange term
D_{mo}	1 (cm^2/h)	Diffusion coefficient
λ_{mL}, λ_{mT}	15, 1.5 (cm)	Longitudinal, tranverse dispersivity

[a] USDA (1998).
[b] Logsdon (2002), Casey et al. (1997, 1998, 1999) and Jaynes et al. (1995).

the mobile domain, θ_{rm} and the values for λ_T, λ_L, and D_0 (Table 1). The value of θ_{rm} was held constant at 0. The values of λ_T and λ_L were kept at fairly high values to account for heterogeneity in the large field domain and to help maintain numerical stability. The value of D_0 was also high, though its effect on the overall dispersion coefficient is likely to be dominated by hydrodynamic dispersion. The potential values of the other model parameters were only weakly constrained to be within a realistic range based on literature values (Table 1). For parameters, where literature references were unavailable or inconclusive, a relatively wide range of values was permitted to account for the non-ideal behavior of macroporous soils. In particular, ω_w was permitted to fluctuate from relatively large values, as would be expected for short transport lengths and large macropore conductivities to small values that might result from clay-organic coatings on the interfaces between the soil matrix and the macropores (Gerke and van Genuchten, 1993). By not rigidly constraining parameter ranges, non-unique parameter sets are possible, especially with the large number of terms in each model. The possibility of non-uniqueness is further addressed in the discussion of the modeling results. Following the calibration of all water flow parameters, the value of ω_s was adjusted separately for chloride and bromide during the solute flux simulations.

The numerical simulations for solute flux coupled with water flow were analogous to the simulations with water flux alone except that the finite-element grid was refined to 86×53 finite elements (rather than the 60×43 grid used in the water flux study) in order to obtain acceptable mass-balance errors for the solutes. The solute applications were simulated by specifying an initial solute concentration to the mesh elements approximately corresponding to the top 2 cm of the domain.

Each solute simulation was first run using the effective parameters estimated from the water flow simulations, and from these model runs, ω_s was adjusted based on the cumulative solute flux data (measured solute concentration multiplied by the measured water flow). Following these simulations, effective parameters were recalibrated based solely on the cumulative solute flux. The purpose of calibrating

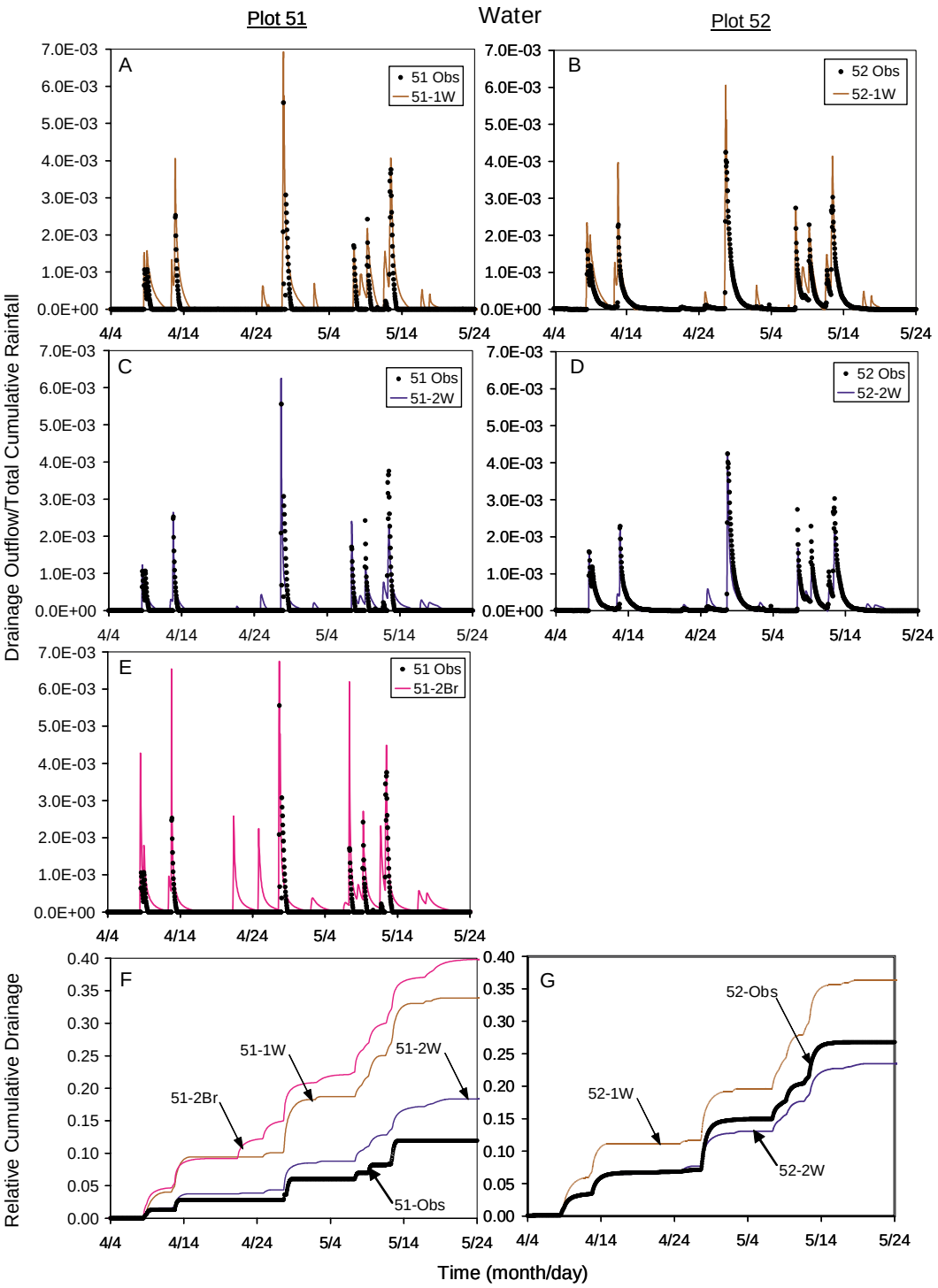

Fig. 3. Simulated (single-porosity [1W], dual-porosity [2W], and dual-porosity with parameters calibrated from bromide flux [2Br]) and observed normalized water fluxes for Plots 51 and 52. Cumulative normalized water fluxes shown in (E) and (F).

based on solute flux was to further constrain the inverse solution because the solute flux data comprised both the water flux data and the measured solute concentrations. Due to the lengthy simulation times, only the dual-porosity model for Plot 51 was investigated for this part of the study. Plot 51 was chosen for these simulations because of the greater confidence in the accuracy of the estimates of the background chloride concentration (see Section 4 below). In this re-calibration of parameter values, the effective parameter values calibrated in the water flow data were used as the initial parameter estimates. Initially, K_s, θ_{sm}, and ω_w were calibrated with the other parameters held constant; then, θ_{sim} and the van Genuchten (1980) parameters in both regions were calibrated before a final adjustment of ω_w. The calibration period for chloride and bromide was maintained as defined for the water flux simulations; however, an additional constraint was imposed for the bromide calibration in that the initial breakthrough of the simulation had to also correspond with the observed initial bromide breakthrough. As will be demonstrated, this additional constraint was incorporated due to the difficulty in reproducing the initial arrival of bromide in the drain outflow.

4. Results

4.1. Hydrograph simulations using effective parameters computed from water flux

Both the single-porosity and dual-porosity simulations successfully capture the main attributes of the flow hydrographs for Plots 51 and 52 (Fig. 3(A)–(D)). The correlation between simulated and observed hydrographs is generally better for Plot 52 than 51, as reflected in the values of ρ_{xy} that are above 0.9 for the validation period for Plot 52 and only 0.75 and 0.72 for the single- and dual-porosity model simulations, respectively, for Plot 51 (Table 2). One apparent reason for the stronger correlation with the Plot 52 hydrograph is the difficulty in simulating a sharp, high peak flow followed by a short recession limb. Since the peaks are generally smaller and the recession limbs longer in Plot 52, the simulations of drainage outflow in Plot 52 fit the observed data better. The sharp peaks and short recessions are indicative of flow through macropores that dominate the drainage response. Macropores quickly convey water to the drain outlet upon filling, and then rapidly drain as the soil becomes even slightly unsaturated (e.g. Mohanty et al., 1996). That the simulations have difficulty matching this response is illustrated in the large over-predictions of the cumulative discharge (Fig. 3(F) and (G)) and manifests a deficiency in representing the field-scale flow processes. The over-predictions of cumulative discharge in the latter part of the simulations also may be due, in part, to a discrepancy in the water budget during May. Yet, this discrepancy in the water budget is reconciled by the end of May while the over-predictions in the cumulative water fluxes continue to increase throughout the duration of the simulation, indicative of a consistent failure in the simulations to match the rapid drainage recessions of the measured outflows.

Table 2
Correlation coefficients and sum of squared deviations for water flow in single-porosity simulations (1W), dual-porosity simulations (2W) and dual-porosity simulation using parameters calibrated from bromide flux (2Br)

Simulation	Correlation coefficient (ρ_{xy})		Sum of squared deviations (SSD)	
	Calibration	*Validation*	*Calibration*	*Validation*
51-1W	0.82	0.75	5.6×10^{-5}	2.6×10^{-4}
51-2W	0.94	0.72	5.6×10^{-6}	1.2×10^{-4}
52-1W	0.91	0.92	3.8×10^{-5}	8.7×10^{-5}
52-2W	0.98	0.94	3.8×10^{-6}	4.7×10^{-5}
51-2Br	0.56	0.64	1.6×10^{-4}	4.0×10^{-4}

The single-porosity and the dual-porosity simulations have a comparable ability to predict the timing and shape of the outflow hydrographs - manifested by their similar values of ρ_{xy} (Table 2); however, the superiority of the dual-porosity model is evident in comparison to the single-porosity model because of its ability to more closely match peak discharge values and recession limbs. The θ_{sm} value of the dual-porosity model (Table 3) permits an abrupt termination in the recession limbs, and water exchange between the mobile and immobile regions allows water to be stored within the flow domain so a water balance can be met without prolonged flow through the subsurface drain. The advantage of the dual-porosity model in replicating both the hydrograph behavior and the cumulative drainage is reflected in

Table 3
Calibrated parameters from HYDRUS-2D inverse modeling of water flow data

	Mobile domain					Immobile domain					
	θ_{rm}	θ_{sm}	α_m (cm^{-1})	n_m	K_s (cm/h)	θ_{rim}	θ_{sim}	α_{im} (cm^{-1})	n_{im}	ω_w (h^{-1})	ω_s (h^{-1})
51-1W	0.25	0.40	0.010	1.75	6.0	–	–	–	–	–	–
51-2W	0	0.073	0.036	1.30	4.8	0.10	0.30	0.020	6.0	5.0×10^{-5}	2.5×10^{-4}[a]
52-1W	0.25	0.40	0.010	1.75	5.0	–	–	–	–	–	–
52-2W	0	0.070	0.032	1.51	3.6	0.10	0.50	0.016	6.0	1.6×10^{-5}	1.5×10^{-3}[a]
51-2Br	0	0.035	0.01	1.30	25	0.1	0.4	0.01	6.0	1.75×10^{-4}	5.4×10^{-2}[a]
Sand	0.05	0.43	0.15	2.68	30	–	–	–	–	–	–
SCLoam	0.09	0.43	0.01	1.23	0.07		–	–	–	–	–

Typical values, estimated from the Rosetta database (Schaap, 1999), for sand and silty-clay loam (SCLoam) are given for comparison.
[a] This value was used only for the chloride flux simulations. For all simulations of the bromide flux, $\omega_s=0$.

the SSD values of the dual- porosity simulations that are a full order of magnitude smaller than the single-porosity simulations for the calibration period and about twice as small for the validation period (Table 2).

Despite the good reproduction of the main hydrograph features, the values of the effective parameters (Table 3) cast ambiguity on how well these parameters physically represent the flow domain. The fitted values for the saturated hydraulic conductivity (Table 3) are in the range of, though in general much lower than (by a factor of 2–3 times in some cases) steady-state infiltration rates measured for macroporous soils at a nearby location (Haws et al., 2004). The precipitation events had rainfall intensity rates lower than the calibrated K_s value resulting in a calibrated value beyond the direct measurement range. Still, these smaller-than-expected values for the hydraulic conductivity, while not unrealistic, do raise concern regarding the uniqueness and physical meaning of the parameters.

The values for van Genuchten (1980) parameters in the mobile and immobile domains are also unexpected. In theory, the water content in macropores should rapidly drain to a residual value at small tensions, resulting in a hydraulic conductivity function that almost immediately decreases from an extremely large saturated value to 0 (Logsdon and Jaynes, 1993; Mohanty et al, 1996, 1997). These macropore characteristics are comparable to the drainage behavior of coarse sand. In contrast, the water release characteristics of the soil matrix regions should better mimic silty-clay loam soil, having a much slower release of water and retaining a relatively high degree of saturation at large tension values. The more non-linear water retention and hydraulic conductivity functions of sands are represented in the van Genuchten (1980) model with larger values of α and n, such that these parameters would be expected to be greater for the macropore domain in comparison to the soil matrix. The optimized α values are, as expected, larger for the mobile domain than for the immobile domain; yet in contrast to intuition, the calibrated n parameter exhibits the opposite trend (Table 3, Fig. 4). For the dual-porosity simulations, the n parameter is smaller for the mobile (macropore) regions and larger for the immobile (clayey) domain. A possible reason that these n parameters are able to reproduce the observed water flow is that the van Genuchten (1980) model cannot accurately describe the characteristic curve for macropores at pressure heads near saturation (De Vos et al., 1997; Mohanty et al., 1997). This near-saturation region, though a relatively small portion of the full range of pressure heads encountered in the simulation (0 to −400 cm), would govern the flow of water during the major rainfall events. Due to the location of the drain at 100 cm below the soil surface and the fluctuation of the groundwater level above this depth, the pressure heads encountered in the soil profile are mostly between 0 and −100 cm. In the simulations, only in the narrow soil surface layer (≧30 cm depth) did the calculated pressure heads drop below −100 cm. Therefore, the parameter calibrations are dominated by the flow events in the narrow pressure head range between 0 and −100 cm.

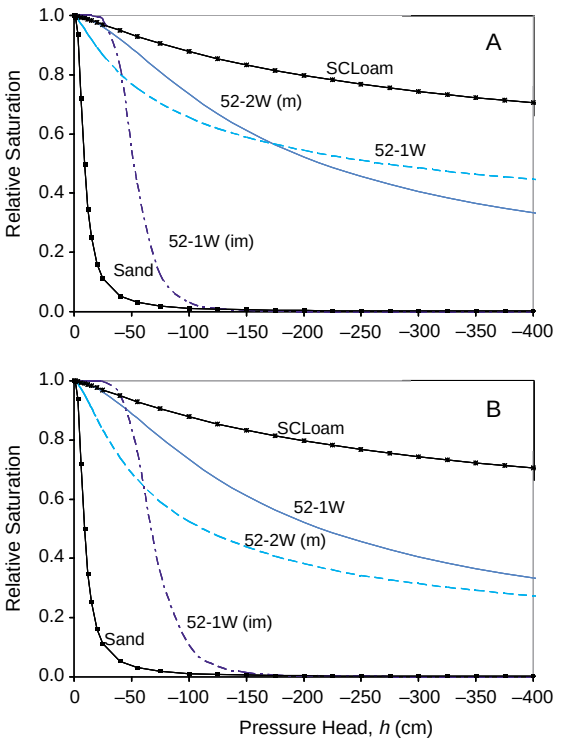

Fig. 4. Water retention characteristics from the soil hydraulic parameters estimated from the inverse modeling for (a) Plot 51 and (b) Plot 52.

Within this range the calibrated parameters produce water retention curves that would be expected for mobile and immobile regions, i.e. with the effective saturation being larger for the immobile domain as compared to the mobile domain for the same pressure heads (Fig. 4).

Another likely reason for the large n values of the soil matrix region is the possibility of correlations between the parameters. With nine parameters in the dual-porosity calibration (or 10 if θ_{rm} is not set to 0), there is a high likelihood of correlation. Hence, a small hydraulic conductivity might be compensated by unrealistic values of the other parameters. The n parameter is often found to be correlated with other soil hydraulic parameters, mainly K_s and θ_r (Šimůnek and van Genuchten, 1996; Šimůnek et al., 1998). Consequently, an impressive hydrograph fit could be achieved by artificially relegating the storage and release of water rather than matching the actual internal flow and transport pathways within the integrated hydrologic system.

4.2. Solute simulations using effective parameters computed from water flux

The simulations of the chloride fluxes further show the superiority of the dual-porosity model over the single-porosity model. The dual-porosity simulations better match the general timing and shape of the chloride fluxes, particularly after the first event (Fig. 5(A)–(D)), resulting in reasonable ρ_{xy} values of 0.67 for Plot 51 and 0.50 for Plot 52 (Table 4). Because the dual-porosity model can transport water and solute through a small fraction of the total domain and also transfer water to, and store water in, the soil matrix, it can produce higher transport velocities (i.e. shorter peak arrival times) with smaller overall water and solute mass flux than the single-porosity model.

Despite the reasonable chloride predictions with the dual-porosity simulations, the solute flux simulations reveal many of the inadequacies of the effective parameters that were not apparent in the water outflow simulations. Even though the initial arrival of chloride is predicted well and early cumulative fluxes are only slightly under-predicted, it appreciably over-predicts the cumulative chloride fluxes in both plots after the calibration period (Fig. 5(F) and (G)). Again, some of this over-prediction may be attributable to the potential under balance in the water budget during May. However, the initial slight under-prediction of chloride fluxes followed by large over-predictions indicates that the simulated mean arrival time for chloride is later than in the field.

Model deficiencies are more evident with the bromide simulations (Fig. 6). The simulated bromide breakthrough curves for both the single- and dual-porosity models significantly lag the observed bromide fluxes. The simulations with the single-porosity model never show bromide breakthrough, and even the dual-porosity simulations do not predict bromide breakthrough until the final drainage event. Virtually no correlation is evident between observed and simulated results (Table 4). It should be noted that the experimental data for Plot 52 show a slightly larger relative amount of bromide drained than of chloride (compare Figs. 5(G) and 6(D)). This is likely

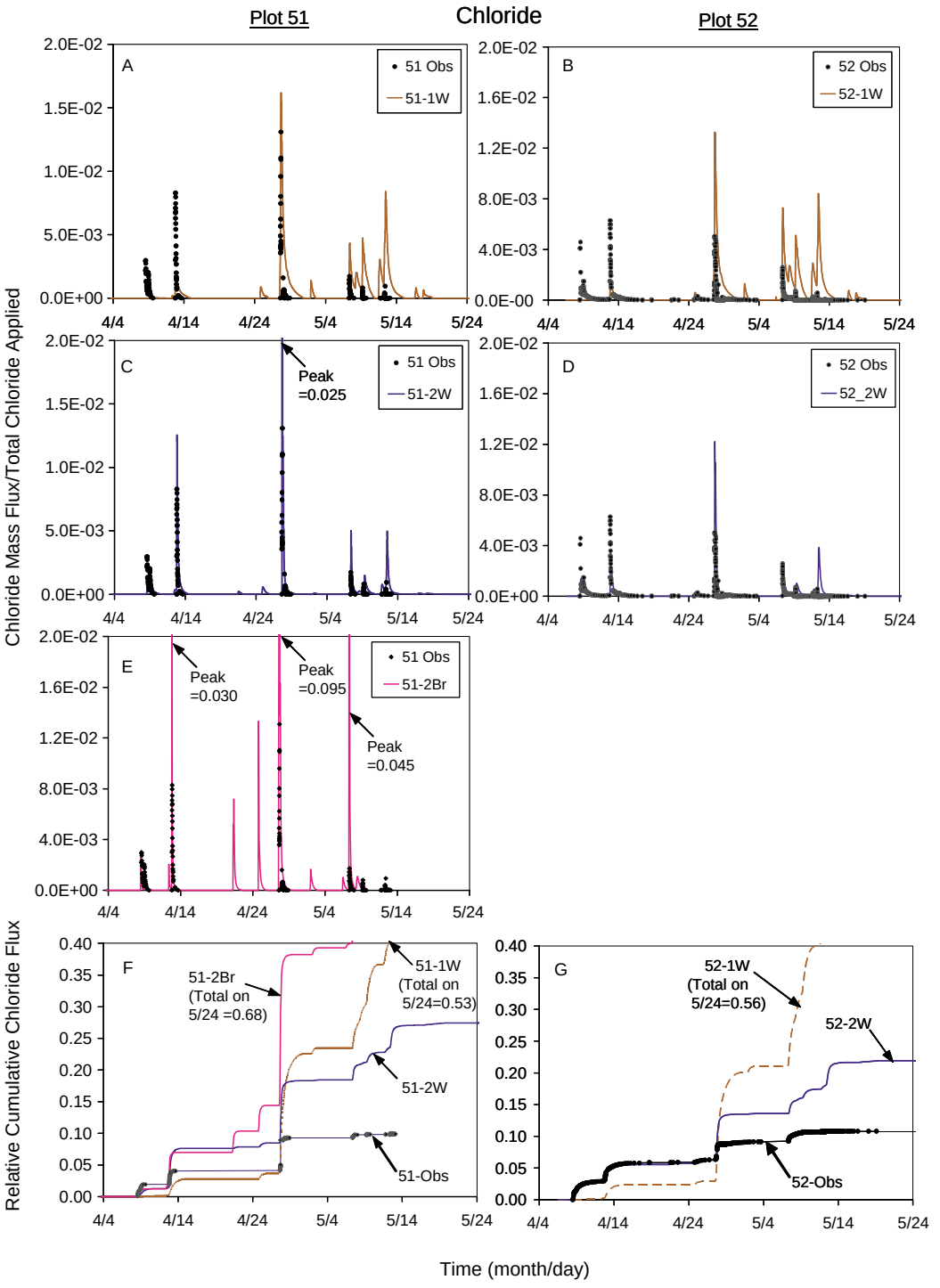

Fig. 5. Simulated (single-porosity [1W], dual-porosity [2W], and dual-porosity with parameters calibrated from bromide flux [2Br]) and observed chloride mass flux for Plots 51 and 52. Cumulative chloride flux shown in shown in (E) and (F).

Table 4
Correlation coefficients and sum of squared deviations statistics for solute transport simulations using effective parameters calibrated from water flow for single-porosity simulations (1W) dual-porosity simulations (2W) and dual-porosity simulation using parameters calibrated from bromide flux (2Br)

Simulation	Correlation coefficient (ρ_{xy})		Sum of squared deviations (SSD)	
	Chloride	Bromide	Chloride	Bromide
51-1W	0.27	0.054	3.7×10^{-3}	2.7×10^{-4}
51-2W	0.67	0.069	6.1×10^{-3}	2.4×10^{-4}
52-1W	0.38	−0.13	9.1×10^{-3}	5.2×10^{-4}
52-2W	0.50	−0.12	2.2×10^{-3}	1.3×10^{-3}
52-2Br	0.70	−0.18	1.1×10^{-3}	2.8×10^{-2}

due to an overestimation of the background chloride concentration in Plot 52. While it was not expected that a model based on the assumption of homogeneity and effective properties would be able to reproduce a larger cumulative chloride flux than bromide, the inability to match the bromide breakthrough time clearly evidences that the models do not accurately capture the internal flow and transport processes even though they provided good matches with the observed water flux.

These findings are comparable with those of previous studies. In the study of De Vos et al. (1997), solute arrival times predicted using effective parameters for a single-porosity model were

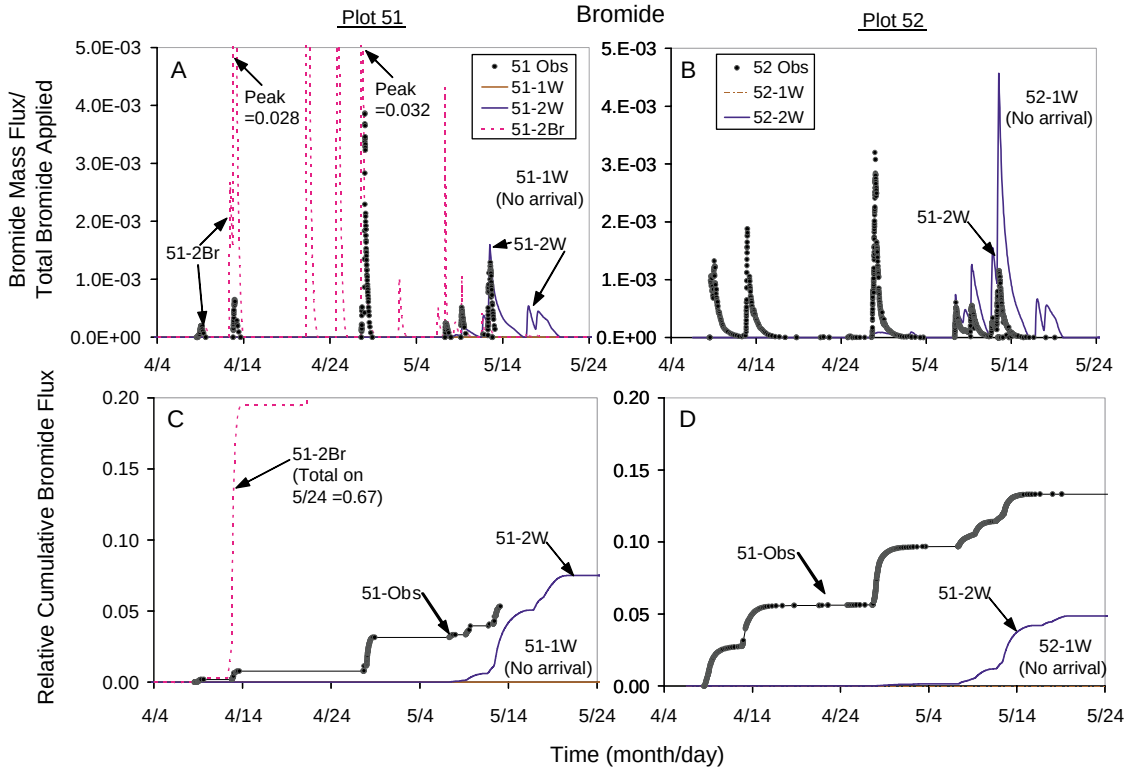

Fig. 6. Simulated (single-porosity [1W], dual-porosity [2W], and dual-porosity with parameters calibrated from bromide flux [2Br]) and observed bromide mass flux for Plots 51 and 52. Cumulative chloride flux shown in (C) and (D).

considerably later than the observed results. The authors surmised that significant improvement could be made using a dual-domain model. Later, Gerke and Köhne (2004) demonstrated that a dual-domain model can improve the prediction of solute arrival times. Though, in the present study, the dual-porosity model does perform better than the single-porosity model, the overall failure of both models implies that a homogeneous, two-dimensional representation cannot adequately capture the complex flow and transport pathways of a heterogeneous three-dimensional domain. Specifically, the lag in the simulated bromide breakthrough in this study indicates that the areas contributing water to outflow drainage in the actual field plots are much greater than those of the simulated transport domains. This discrepancy precludes affixing a rigid physical basis to the effective parameters since they were essentially calibrated across different spatial support areas as opposed to what contributed to the drainage outflow measured in the subsurface drains. Hence, even though the effective parameter models did successfully predict water flow, it must be conceded that the parameters themselves are simply empirical fits.

4.3. Effective parameters derived from solute data

The parameters from the inverse optimization using the cumulative solute flux are included with the parameters for calibration using only water flow data in Table 3. In the calibration using the cumulative chloride flux, no improvement could be made over the parameters calibrated from the water flux (51–2 W). Therefore, Table 3 does not report any additional parameters for the chloride flux calibration. In the calibration using the cumulative bromide flux, the values of θ_{sm}, α_s, K_s, and ω_w were most dramatically altered (Table 3). As expected, the value of θ_{sm} decreased and the value of K_s increased to allow increased transport velocities. The increase in ω_w may be partly due to correlations with changes in the water retention parameters.

The simulations using the calibrated parameters based on cumulative bromide flux reproduce the initial arrival of the applied bromide exceptionally well. However, after the first drainage event, bromide flux is dramatically over-predicted (Fig. 6(C)). In addition, the simulated total water flow is over four times greater than observed for the water flux-based parameter simulations (Fig. 3(F)). Thus, the rapid bromide arrival is reproduced only by increasing the water flux and not by accurately simulating the field preferential flow and dual-domain transport processes. Before separately adjusting the value of ω_s for chloride, the chloride flux simulations, using the effective parameters calibrated from the bromide flux data, dramatically over-predicted the observed flux for all events. The simulated chloride flux is kept close to the observed chloride flux for the first event only after adjusting ω_s for chloride to a very large value ($0.054\ h^{-1}$). However, after the calibration period, where the simulated chloride flux is greater than the observed flux (Fig. 5(E) and (F)), the large difference in the value of ω_s for two similar solutes placed on the same field is further indication that the parameters lack the ability to mechanistically explain the complicated multi-domain processes.

5. Discussion and conclusions

The failure of the single-porosity model, and even the dual-porosity model, to simultaneously predict both water and solute flux at the subsurface drain outlet using effective parameters can be credited to several factors other than the underlying conceptual models. A more rigorous and better-constrained inverse procedure may have improved parameter optimization. Specifically, the simultaneously fitting of nine parameters is prone to correlated parameters, non-unique solution sets, and local minima in the objective function (Hopmans and Šimůnek, 1997). In addition, the final calibrated values for the hydraulic parameters were certainly influenced by the initial parameter estimates. Thus, it should be stressed that the inability to calibrate realistic parameter values does not implicate a failure in the conceptual model per se.

Beyond the limitations of the calibration procedure, however, a fundamental issue contributing to the deficiencies of the simulations is imposing homogeneity on a domain, where flow and transport is highly dependent on the geomorphology of intrinsic preferential networks. Disregard of preferential pathways often leads to significant disagreement between the simulated and observed solute arrival times

(Grayson and Bloschl, 2000) because preferential pathways likely 'short-cut' the flow lines predicted from a Richards-based model. This shortcutting of 'ideal' pathways may also explain why chloride was better simulated than bromide. With chloride placed almost directly over the drain, its modeled and actual streamlines would both be fairly unidirectional and thus have less pronounced differences than those for bromide, whose 'ideal' streamlines would be longer and more curvilinear, and therefore, more susceptible to short-cutting. Similarly, this indicates why a dual-domain model might satisfactorily simulate solute transport in a one-dimensional flow domain, where short-cutting is not manifested, but fail to predict solute arrival in a two-dimensional domain, where short-cutting can be important.

The over-prediction of water flow in the simulations using parameters calibrated from bromide flux data further highlight the misrepresentation of the true field processes. The shortcutting of the ideal streamlines results in quick water and solute arrival times with relatively little drainage. Because even the homogeneous dual-porosity model transports water and solute through ideal streamlines, it can only match the observed solute fluxes by flushing a larger volume of water. The observed rapid arrival times with relatively little water drainage also suggest a smaller saturated mobile water content, θ_{sm}, than used in the effective parameter simulations. Although the θ_{sm} values used in the simulations agreed with field-measured values, recent studies report that the continuous macropore fraction contributing to the outflow response may be much less than values measured at the soil surface (Jorgensen et al., 2002; Deurer et al., 2003).

A general conclusion of this study is that a model's success or failure to represent the flow and transport processes internal to the transport domain should not be judged solely by the response prediction at a single outlet point. As demonstrated in this study, parameters that produced a seemingly good hydrograph fit may not accurately predict solute fluxes (representative of internal transport pathways). Thus a good hydrograph fit does not denote a physical meaning of the model parameters. Extrapolating the significance of a model's success in predicting flow at an outlet point should be exercised with caution.

Acknowledgements

Sincere appreciation is expressed to Dr M. T. van Genuchten at the USDA Soil Salinity Laboratory, Riverside, CA for his encouragement to use dual-porosity models for field-scale applications. The authors also thank Dr Sylvie Brouder and Jim Beaty in the Department of Agronomy at Purdue University for providing access to the Water Quality Field Station.

References

Baveye, P., Sposito, G., 1984. The operational significance of the continuous hypothesis in the theory of water movement through soils and aquifers. Water Resour. Res. 20 (5), 521–530.

Beran, M., 1999. Hydrograph prediction—how much skill? Hydrol. Earth Syst. Sci. 3 (2), 305–337.

Berkowitz, B., Bear, J.C., Braester, C., 1988. Continuum models for contaminant transport in fractured porous media. Water Resour. Res. 24 (8), 1225–1236.

Beven, K., 1993. Prophecy, reality and uncertainty in distributed hydrological modeling. Adv. Water Resour. 16 (1), 41–551.

Binley, A.M., Beven, K., Calver, A., Watts, L.G., 1991. Changing responses in hydrology—assessing the uncertainty in physically based model predictions. Water Resour. Res. 27 (6), 1253–1261.

Blazkova, S., Beven, K., Tacheci, P., Kulasova, A., 2002. Testing the distributed water table predictions of Topmodel (allowing for uncertainty in model calibration): the death of Topmodel? Water Resour. Res. 38 (11) (Art. no. 1257).

Brouwer, C., Heibloem, M., 1986. Irrigation water management, training manual no. 3: irrigation water needs, Food and Agricultural Organization of the United Nations, Rome, Italy 1986.

Casey, F.X.M., Logsdon, S.D., Horton, R., Jaynes, D.B., 1997. Immobile water content and mass exchange coefficient in a field soil. Soil Sci. Soc. Am. J. 61, 1030–1036.

Casey, F.X.M., Logsdon, S.D., Horton, R., Jaynes, D.B., 1998. Measurement of field hydraulic and solute transport parameters. Soil Sci. Soc. Am. J. 62, 1172–1178.

Casey, F.X.M., Logsdon, S.D., Horton, R., Jaynes, D.B., 1999. Comparing field methods that estimate mobile–immobile model parameters. Soil Sci. Soc. Am. J. 63, 800–806.

Deurer, M., Green, S.R., Clothier, B.E., Bottcher, J., Duijnisveld, W.H.M., 2003. Drainage networks in soils. A concept to describe bypass-flow pathways. J. Hydrol. 272, 148–162.

De Vos, J.A., Simunek, J., Raats, P.A.C., Feddes, R.A., 1997. Identification of the hydraulic characteristics of a layered silt loam. In: van Genuchten, Th, M., Leij, F.J., Wu, L. (Eds.), Characterization and Measurement of Hydraulic Properties of Unsaturated Porous Media. University of California, Riverside, CA, pp. 783–798.

Doherty, J., Johnston, J.M., 2003. Methodologies for calibration and predictive analysis of a watershed model. J. Am. Water Resour. Assoc. 39 (2), 251–265.

Durner, W., Schultz, B., Zurmühl, T., 1997. State-of-the-art in inverse modeling of inflow/outflow experiments. In: van Genuchten, Th, M., Leij, F.J., Wu, L. (Eds.), Characterization and Measurement of Hydraulic Properties of Unsaturated Porous Media. University of California, Riverside, CA, pp. 661–682.

Fernandez-Garcia, D., Sanchez-Vila, X., Illangasekare, T.H., 2002. Convergent-flow tracer tests in heterogeneous media: combined experimental-numerical analysis for determination of equivalent transport parameters. J. Contam. Hydrol. 57, 129–145.

Fipps, G., Skaggs, W.R., Neiber, J.L., 1986. Drains as boundary conditions in finite elements. Water Resour. Res. 22 (11), 1613–1621.

Gerke, H.H., Köhne, J.M., 2004. Dual-permeability modeling of preferential bromide leaching from a tile-drained glacial till agricultural field. J. Hydrol. 289, 239–257.

Gerke, H.H., van Genuchten, M.T., 1993. Evaluation of a first-order water transfer term for variably saturated dual-porosity flow models. Water Resour. Res. 29 (4), 1225–1238.

Gerke, H.H., van Genuchten, M.T., 1996. Macroscopic representation of structural geometry for simulating water and solute movement in dual-porosity media. Adv. Water Resour. 19 (6), 343–357.

Grayson, R., Bloschl, G., 2000. Spatial processes, organisation and patterns. Spatial patterns in catchment hydrology: observations and modeling. In: Grayson, R., Bloschl, G. (Eds.), Spatial Patterns in Catchment Hydrology: Observations and Modelling. Cambridge University Press, Cambridge, UK, pp. 3–16.

Haws, N.W., Liu, B., Boast, C.W., Rao, P.S.C., Kladivko, E.J., Franzmeier, D.P., 2004. Spatial variability and measurement scale of infiltration rate on an agricultural landscape. Soil Sci. Soc. Am. J. 68, 1818–1826.

Hoffman, G.J., Schwab, G.O., 1964. Tile spacing prediction based on drain outflow. Trans. ASAE 7, 444–447.

Hopmans, J.W., Šimůnek, J., 1997. Review of inverse estimation of soil hydraulic properties. In: van Genuchten, Th, M., Leij, F.J., Wu, L. (Eds.), Characterization and Measurement of Hydraulic Properties of Unsaturated Porous Media. University of California, Riverside, CA, pp. 643–660.

Indelman, P., 2002. On mathematical models of average flow in heterogeneous formations. Transport Porous Media 48, 209–224.

Jacques, D., Feyen, J., Mallants, D., 1997. Determination of hydraulic properties using tension infiltrometer data and inverse optimization. In: van Genuchten, Th, M., Leij, F.J., Wu, L. (Eds.), Characterization and Measurement of Hydraulic Properties of Unsaturated Porous Media. University of California, Riverside, CA, pp. 749–760.

Jain, S.K., Storm, S.B., Bathurst, J.C., Refsgaard, J.C., Singh, R.D., 1992. Application of the SHE to catchments in India. Part 2. Field experiments and simulation studies with SHE or the kolar subcatchment of the Naramada river. J. Hydrol. 140, 25–47.

Jaynes, D.B., Logsdon, S.D., Horton, R., 1995. Field method for measuring mobile/immobile water content and solute transfer rate coefficient. Soil Sci. Soc. Am. J. 59, 352–356.

Jorgensen, P.R., Hoffman, M., Kistrup, J.P., Bryde, C., Bossi, R., Villholth, K.G., 2002. Preferential flow and pesticide transport in a clay-rich till: field, laboratory, and modeling analysis. Water Resour. Res. 38 (11), 1246.

Logsdon, S.D., 2002. Determination of preferential flow model parameters. Soil Sci. Soc. Am. J. 66, 1095–1103.

Logsdon, S.D., Jaynes, D.B., 1993. Methodology for determining hydraulic conductivity with tension infiltrometers. Soil Sci. Soc. Am. J. 57, 1426–1431.

Lugo, J.E., Rio, J.A.D., Taguena-Martinez, J., 1998. Influence of nonlinear local properties on effective transport. Transport Porous Media 31, 89–108.

Madsen, H., Wilson, G., Ammentorp, H.C., 2002. Comparison of different automated strategies for calibration of rainfall-runoff models. J. Hydrol. 261 (1–4), 48–59.

Mohammad, F.S., Skaggs, W.R., 1983. Drain tube opening effects on drain inflow. Irrig. Drain. Div., Am. Soc. Civ. Eng. 109 (4), 393–404.

Mohanty, B.P., Horton, R., Ankeny, M.D., 1996. Infiltration and macroporosity under a row crop agricultural field in a glacial till soil. Soil Sci. 169 (4), 205–213.

Mohanty, B.P., Bowman, R.S., Hendrickx, J.H.M., van Genuchten, M.T., 1997. New piecewise-continuous hydraulic functions for modeling preferential flow in an intermittent-flood-irrigated field. Water Resour. Res. 33 (9), 2049–2063.

Neuman, S.P., Orr, S., 1993. Prediction of steady state flow in nonuniform geologic media by conditional moments: exact nonlocal formalism, effective conductivities, and weak approximation. Water Resour. Res. 29 (2), 341–364.

Royer, P., Auriault, J.-L., Lewandowska, J., Serres, C., 2002. Continuum modelling of contaminant transport in fractured porous media. Transport Porous Media 49, 333–359.

Schaap, M., 1999. Rosetta Help File. US Salinity Laboratory, Riverside, CA.

Šimůnek, J., van Genuchten, M.T., 1996. Estimating unsaturated soil hydraulic properties from tension disc infiltrometer data by numerical inversion. Water Resour. Res. 32 (9), 2683–2696.

Šimůnek, J., Wendroth, O., van Genuchten, M., Th, A., 1998. A parameter estimation analysis of the evaporation method for determining soil hydraulic properties. Soil Sci. Soc. Am. J. 62 (4), 894–905.

Šimůnek, J., Sejna, M., van Genuchten, M.T., 1999. The HYDRUS-2D software package for simulating the two-dimensional movement of water, heat, and multiple solutes in variably saturated media. Version 2.0, IGWMC-TPS-53, International Groundwater Modeling Center, Colorado School of Mines, Golden, CO.

Šimůnek, J., Jarvis, N.J., van Genuchten, M.T., Gardenas, A., 2003. Review and comparison of models for describing nonequilibrium and preferential flow and transport in the vadose zone. J. Hydrol. 272, 14–35.

Skaggs, W.R., 1976. Determination of the hydraulic conductivity—drainable porosity from water table measurements. Trans. ASAE 19, 73–84.

Tartakovsky, D.M., Neuman, S.P., 1998a. Transient flow in bounded randomly heterogeneous domains 1. Exact conditional moment equations and recursive approximations. Water Resour. Res. 34 (1), 1–12.

Tartakovsky, D.M., Neuman, S.P., 1998b. Transient flow in bounded randomly heterogeneous domains 2. Localization of

conditional mean equations and temporal nonlocality effects. Water Resour. Res. 34 (1), 13–20.

Tartakovsky, D.M., Neuman, S.P., 1998c. Transient effective hydraulic conductivities under slowly and rapidly varying mean gradients in bounded three-dimensional media. Water Resour. Res. 34 (1), 21–32.

United States Department of Agriculture (USDA), 1998. Soil survey of Tippecanoe county, Indiana. Purdue University Agricultural Experiment Station, Indiana. Indiana Department of Natural Resources, State Soil Conservation Board and the Division of Soil Conservation. West Lafayette, Indiana.

van Genuchten, M.T., 1980. A closed-form equation for predicting the hydraulic conductivity of unsaturated soils. Soil Sci. Soc. Am. J. 44, 892–898.

Yeh, T.-C.J., 1997. A site characterization method for the vadose zone. In: van Genuchten, Th, M., Leij, F.J., Wu, L. (Eds.), Characterization and Measurement of Hydraulic Properties of Unsaturated Porous Media. University of California, Riverside, CA, pp. 1377–1380.